IOP PUBLISHING NANOTECHNOLOGY

Nanotechnology **21** (2010) 105710 (8pp) doi:10.1088/0957-4484/21/10/105710

On the utility of vacancies and tensile strain-induced quality factor enhancement for mass sensing using graphene monolayers

Sung Youb Kim[1] **and Harold S Park**[2]

[1] School of Mechanical Engineering, Ulsan National Institute of Science and Technology,
Ulsan 689-798, Korea
[2] Department of Mechanical Engineering, University of Colorado, Boulder, CO 80309, USA

E-mail: parkhs@bu.edu

Received 24 September 2009, in final form 9 January 2010
Published 16 February 2010
Online at stacks.iop.org/Nano/21/105710

Abstract

We have utilized classical molecular dynamics to investigate the mass sensing potential of graphene monolayers, using gold as the model adsorbed atom. In doing so, we report two key findings. First, we find that while perfect graphene monolayers are effective mass sensors at very low ($T < 10$ K) temperatures, their mass sensing capability is lost at higher temperatures due to diffusion of the adsorbed atom at elevated temperatures. We demonstrate that even if the quality (Q) factors are significantly elevated through the application of tensile mechanical strain, the mass sensing resolution is still lost at elevated temperatures, which demonstrates that high Q-factors alone are insufficient to ensure the mass sensing capability of graphene. Second, we find that while the introduction of single vacancies into the graphene monolayer prevents the diffusion of the adsorbed atom, the mass sensing resolution is still lost at higher temperatures, again due to Q-factor degradation. We finally demonstrate that if the Q-factors of the graphene monolayers with single vacancies are kept acceptably high through the application of tensile strain, then the high Q-factors, in conjunction with the single atom vacancies to stop the diffusion of the adsorbed atom, enable graphene to maintain its mass sensing capability across a range of technologically relevant operating temperatures.

(Some figures in this article are in colour only in the electronic version)

1. Introduction

Graphene has recently been discovered as the simplest two-dimensional crystal structure [1, 2], and has been found to have a variety of exceptional or unusual physical properties [3, 4], many of which have contributed a view of graphene as being one of the key building blocks for future nanoelectromechanical systems (NEMS) [5–8].

One of the key applications for graphene is as an ultrasensitive mass sensor, with the potential to detect single atoms or molecules with masses as small as fractions of zeptograms [5]. In this respect, graphene will serve as the next-generation of carbon-based nanosensors, where carbon nanotubes have been investigated as mass sensors for many years [9–13], and where recent experimental work by various researchers [12, 13] has indicated that carbon nanotubes may be utilized to detect individual atoms. We note that other nanomaterials such as nanowires have also been investigated for their mass sensing potential [14–16].

In studying the potential of graphene to act as a high performance nanoscale mass sensor, the key measure of its mass sensing potential is whether it will be possible to observe relatively large shifts in resonant frequency Δf for very small amounts of adsorbed mass Δm. It is currently anticipated that graphene will be able to meet this performance measure for the following reasons. First, graphene can oscillate at high resonant frequencies f_0 due to its high elastic modulus, which was recently measured experimentally to be 1 TPa for a graphene monolayer [17]. Second, graphene sheets have an extremely low mass m_0, on the order of 10^{-21} kg; this combination of high resonant frequency and low mass indicates that graphene should be an ideal choice to serve as ultrasensitive nanometer mass sensors.

The detection of individual atoms using graphene sheets is further thought to be feasible despite the low quality (Q)-factors for graphene, on the order of 2–4000, that have been experimentally reported [5, 7, 18] for both single and multilayer graphene and graphene oxide sheets. The Q-factors of graphene may limit its mass sensing capability because the amount of adsorbed mass Δm that can be detected obeys the following relationship, as written by Ekinci *et al* [19]:

$$\Delta m \approx 2m_0 \left(\frac{b}{Q\omega_0}\right)^{1/2} 10^{-DR/20}, \qquad (1)$$

where DR is the dynamic range of the resonator and b is the bandwidth, or the available frequency range of detection; equation (1) clearly indicates that a higher Q-factor is necessary to detect ever smaller masses.

Therefore, the goal of the present work is to utilize classical molecular dynamics (MD) simulations to examine the potential of monolayer graphene sheets as nanoscale mass sensors by studying their response, i.e. changes in their vibrational frequency, to added mass. To do so, following recent experiments [12] using carbon nanotubes, we study the detection of individual gold atoms. Gold is chosen for multiple reasons; for example it is relatively easy to evaporate experimentally onto carbon-based nanostructures, it is relatively mobile at room temperature on graphite, it does not oxidize, unlike other FCC metals such as copper, and it is relatively non-reactive.

Furthermore, in contrast to heavier biomolecules, the addition of gold atoms to graphene monolayers does not cause significant local variations in the Young's modulus of graphene. As shown by Tamayo *et al* [20], these local stiffness variations due to the attachment of heavy biomolecules can cause even larger variations in the resonant frequency than due to the attached mass, thus complicating the mass sensing analysis. Because we wish to isolate the sensitivity of graphene to added mass, we choose gold atoms, rather than specific biomolecules in the present work.

We also note that previous theoretical studies have studied mass sensing using graphene and CNTs, i.e. [21, 22]. However, because both of these are based upon continuum mechanics studies of the carbon-based structure, the actual atomistic nature of bonding between the adsorbed atom and graphene was not considered, and neither considered the importance of Q-factor engineering on the mass sensing capability.

There are two major results in this work. First, while perfect monolayer graphene sheets are found to be effective mass sensors at very low ($T < 10$ K) temperatures, the mass sensing capability is lost at higher temperatures due to both diffusion of the gold atom coupled with the decrease in Q-factors of graphene with increasing temperature. Second, to reduce the loss in mass sensitivity due to diffusion, we introduce single atom vacancies into the graphene monolayer, which successfully prevents diffusion of the gold atoms due to the significantly enhanced binding energy between gold and single atom vacancies in graphene. However, we find that despite the success at preventing diffusion, the low Q-factors of the defective graphene monolayer at elevated temperatures result in a loss of mass sensitivity. Therefore, we then demonstrate that introduction of single atom vacancies in the graphene monolayer to prevent diffusion at high temperatures, coupled with the application of tensile mechanical strain to enhance the Q-factors of graphene at high temperatures, enables graphene to keep its single atom mass sensing capability across a range of technologically relevant operating temperatures.

2. Numerical examples

We studied the mass sensing potential of graphene using a circular monolayer of graphene with two different sizes. The smaller model had a diameter of 42.6 Å, which consisted of 547 carbon atoms; the larger model had a diameter of 125.4 Å, which consisted of 4886 carbon atoms. For both models, all atoms along the outer edge of the sheet were fixed; this was performed in previous experimental studies [7] and MD calculations [23, 24] which showed that spurious edge modes of vibration are one of the key factors that contribute to the low Q-factors of graphene sheets that have been observed experimentally [5, 7, 18]. These edge modes are eliminated in the MD simulations by constraining the edge atoms not to move, and can be removed experimentally by suspending the graphene sheet over a silicon oxide substrate.

We utilized the second generation Brenner potential (REBO-II) [25] for all carbon–carbon interactions; this potential has been shown to accurately reproduce binding energies, force constants and elastic properties of graphene. For the carbon–gold interactions, we utilized a Lennard-Jones (LJ) potential with potential parameters modified for two cases. For the case where the gold atoms interact with a defect-free graphene sheet, recent experimental studies have shown that the cohesive energy of gold on graphite (0001) surfaces is about 0.40 eV [26, 27]. We therefore modified the LJ potential parameters to be $\sigma_{\mathrm{Au-C}} = 2.9943$ Å, and $\epsilon_{\mathrm{Au-C}} = 0.029\,36$ eV in order to reproduce the cohesive energy of 0.40 eV for gold on perfect graphite.

We also considered the case in which a single atom vacancy was introduced at the center of the graphene sheet, to determine if the adsorption of gold into the vacancy enhances the mass sensing capability. Recent density functional theory (DFT) calculations have found that the cohesive energy of gold in a single defect on the graphite (0001) surface is about 2.62 eV [28]; other DFT calculations have placed this value near 3 eV [29]. For this case, we modified the LJ energy well depth parameter $\epsilon_{\mathrm{Au-C}} = 0.778\,60$ eV to reproduce the 2.62 eV cohesive energy for gold interacting with a single atom vacancy on (0001) graphite. We further justify the usage of the LJ potential for the gold–vacancy interactions as the DFT calculations demonstrated that the density of states between gold and the three defected carbon atoms is strongly localized [28]. Therefore, the modified LJ well depth parameter $\epsilon_{\mathrm{Au-C}} = 0.778\,60$ eV was only utilized

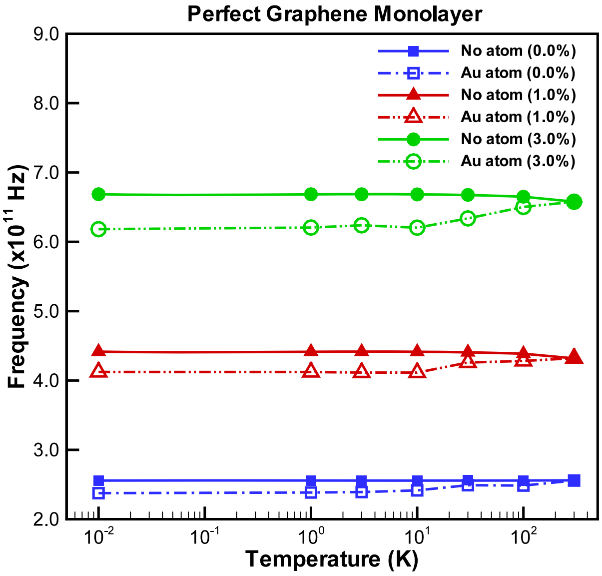

Figure 1. Frequency shift for a perfect graphene monolayer (small model: 547 carbon atoms) for a single adsorbed gold atom at different temperatures and applied tensile strain.

for interactions between gold atoms and the three carbon atoms around the single atom vacancy defect. Gold–gold interactions for multi-atom (three and four atom) gold clusters were modeled using the embedded atom (EAM) potential of Cai and Ye [30].

For all simulations, energy minimizing positions of the graphene monolayer either with or without adsorbed gold atoms were first found. Second, the graphene monolayer either with or without adsorbed gold atoms was equilibrated at a specified temperature using a Nose–Hoover thermostat [31] for 50 000 steps with a 1 fs time step within an *NVT* ensemble. After the thermal equilibration, a sinusoidal velocity profile was applied to the sheet, which had a maximum at the center of the circular sheet, and decayed to zero at the fixed edges of the sheet. After applying the velocity field, the graphene monolayer, either with or without adsorbed gold atoms, was allowed to freely oscillate for 100 000 steps in an energy conserving *NVE* ensemble. The sinusoidal velocity that was applied to induce the oscillations was only 0.016% of the total potential energy of the system, to ensure that nonlinear vibrational modes due to the applied velocity field would not be present.

To calculate the resonant frequency shifts, we calculated the frequencies of oscillation for the graphene monolayer, both with and without the single atom vacancy, and with and without adsorbed atoms for a range of temperatures (0.01, 1, 3, 10, 30, 100, 300 K) and states of applied tensile strain (0%, 1%, 2%, 3%). The strain was applied by symmetrically expanding the circular graphene sheet before the thermal equilibration process, and was utilized as previous MD simulations [23, 24] have demonstrated the utility of mechanical strain in enhancing the Q-factors of graphene monolayers. We note that previous experiments [32], MD simulations [33], and theoretical calculations [34] have all demonstrated that mechanical stress and strain can be used to enhance the Q-factors of both metallic and semiconducting nanowires, as well as carbon nanotubes. Only single adsorbed gold atoms were considered for the perfect graphene monolayer, while one, three, and four adsorbed gold atoms were considered for the defected graphene monolayer. The mass sensitivity measure utilized in the present work for a given temperature and state of strain is the difference in oscillation frequency for the graphene monolayer without adsorbed atoms, and the graphene monolayer with adsorbed atoms.

Table 1. Frequency shift for an unstrained perfect graphene monolayer (small model: 547 carbon atoms). All frequencies are in GHz.

T (K)	No Au atom f_0	One Au atom f_0 (Δf)
0.01	255.73	237.53 (−7.12%)
1	255.76	238.49 (−6.75%)
3	255.80	239.11 (−6.52%)
10	255.45	241.57 (−5.43%)
30	256.00	249.03 (−2.72%)
100	255.68	248.50 (−2.81%)
300	256.04	255.75 (−0.11%)

Table 2. Q-factors for a graphene monolayer (small model: 547 carbon atoms) for different amounts of tensile strain as a function of temperature.

T (K)	Q (0%)	Q (1%)	Q (2%)	Q (3%)
0.01	>1000 000	>1000 000	>1000 000	>1000 000
1	∼800 000	>1000 000	>1000 000	>1000 000
3	∼270 000	>1000 000	>1000 000	>1000 000
10	∼91 000	>1000 000	>1000 000	>1000 000
30	∼45 000	∼500 000	∼600 000	∼1000 000
100	∼12 000	∼160 000	∼340 000	∼480 000
300	∼2 500	∼64 000	∼150 000	∼270 000

2.1. *Perfect graphene monolayer*

We first discuss results for the perfect graphene monolayer, i.e. without the single atom vacancy, to examine its performance as a resonant mass sensor. Figure 1 shows the frequency shift that is obtained for a single gold atom adsorbed on a perfect graphene monolayer for temperatures ranging from near cryogenic (0.01 K) to room temperature (300 K) for the small graphene monolayer (547 carbon atoms) strained between 0% and 3% tensile strain; the actual per cent change in the frequency of oscillation is summarized in table 1.

We also summarize the Q-factors for the graphene monolayer in table 2 for each temperature as a function of applied tensile strain. We emphasize that we found nearly identical Q-factors regardless of whether the graphene monolayer was perfect, or had a single atom vacancy in the center of the monolayer. Because of this, we use the Q-factor values in table 2 interchangeably for both the perfect and defected graphene monolayers. The key point with regards to table 2 is that, for all temperatures, the Q-factors for graphene increase substantially with an increase in applied tensile strain.

The first key point that can be discerned in figure 1 and table 1 is that at low temperatures (T < 10 K), there is a noticeable shift in the frequency of the graphene monolayer

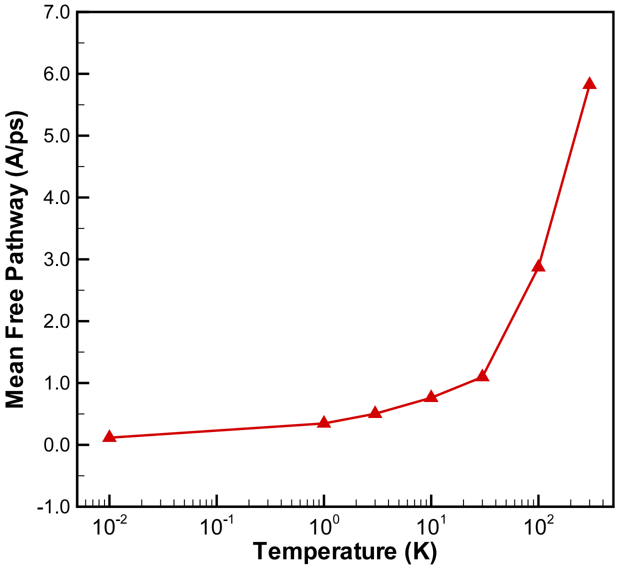

Figure 2. Mean free path of a single gold atom diffusing on the surface of perfect monolayer graphene (large model: 4886 carbon atoms) as a function of temperature.

for a single adsorbed gold atom, where the frequency shift ranges from $\Delta f = -5.5\%$ for unstrained graphene at 10 K to $\Delta f = -7.2\%$ for graphene under a 3% tensile strain at 10 K.

However, for temperatures exceeding 10 K, due to the low binding energy between gold and perfect graphene (0.40 eV), the gold atom begins to diffuse along the graphene surface. This diffusion is reflected in the reduced frequency shift in figure 1 and table 1, which decreases with increasing temperature, where for unstrained graphene the measured frequency shift drops to $\Delta f = -2.7\%$ at 30 K, and then down to $\Delta f = -0.11\%$ at 300 K, which indicates a complete loss of mass sensitivity at room temperature. Figure 1 also demonstrates that at lower temperatures, i.e. $T < 100$ K, the frequency of oscillation is essentially independent of temperature regardless of the amount of tensile strain that is applied to the graphene monolayer, while a slight decrease in the frequency is observed near room temperature.

To further justify our conclusion that diffusion of the gold atom with increasing temperature is responsible for the loss in sensing capability of the graphene monolayer in figure 1, we show in figure 2 the mean free path of a single gold atom on monolayer graphene as a function of temperature. Figure 2 clearly demonstrates that the mean free path for the gold atom increases exponentially with temperature, following the expected Arrhenius-type law. Specifically, the mean free path at 30 K, when the mass sensitivity begins to degrade in figure 1, is about 1.1 Å ps^{-1}, which is nearly ten times larger than the mean free path at 0.01 K.

Furthermore, the mass sensitivity is lost at elevated temperatures regardless of the amount of tensile mechanical strain that is applied to the graphene monolayer. For example, as seen in table 2, when 3% tensile strain is applied, the Q-factor is nearly 270 000, which is 100 times larger than the Q-factor at 0% strain; this should, according to equation (1), significantly enhance the mass sensitivity of the graphene monolayer. Despite the utility of mechanical strain in significantly enhancing the Q-factor, as observed both in the present work and also in previous works on metallic and semiconducting nanowires [23, 32, 35], this increase in Q does not overcome the loss in mass sensitivity due to the diffusion of the gold atom resulting from the lack of strong interatomic bonding between perfect graphene and gold at elevated temperatures. Therefore, we have demonstrated that high Q-factors alone are not sufficient to ensure highly sensitive graphene-based mass sensors.

2.2. Graphene monolayer with single atom vacancy

While the mass sensitivity of perfect graphene was shown to be excellent at low temperatures, a key performance issue for practical graphene-based NEMS applications will be to maintain this mass sensitivity at elevated temperatures, i.e. up to room temperature. Due to the results of section 2.1, which demonstrated that for perfect graphene, the lack of strong bonding between the gold and graphene enabled the diffusion of graphene at elevated temperatures, we now study the potential of graphene monolayers with a single vacancy at the center of the monolayer as an enhanced nanoscale mass sensor. The defect is expected to enhance the mass sensitivity of graphene at high temperature because the cohesive energy of gold to defective carbon atoms as determined by recent DFT calculations is about 2.62 eV [28], which is more than 6.5 times larger than the binding energy of 0.4 eV for gold to perfect graphene [26, 27].

Figure 3 shows the change in frequency for an unstrained graphene monolayer with a single vacancy for one, three, and four adsorbed gold atoms at different temperatures as compared to an unstrained graphene monolayer with a single vacancy and no adsorbed mass; we note that the frequency shift is larger for the small model as expected due to its smaller mass. The results in figure 3 are somewhat surprising, because a loss in mass sensitivity is still observed for all numbers of adsorbed gold atoms for temperatures exceeding about 30 K, for both the small and large graphene monolayers. Furthermore, for the single adsorbed gold atom on the small graphene monolayer in figure 3(a), the loss in mass sensitivity is observed for all temperatures exceeding 0.01 K, i.e. $\Delta f = -7\%$ when $T = 0.01$ K, but decreases to $\Delta f = -5.4\%$ when $T = 3$ K, and decreases even further to $\Delta f = -1.27\%$ when $T = 30$ K; this loss in mass sensitivity is observed even though the single gold atom remains bound to the vacancy in the graphene sheet and thus does not diffuse for all temperatures. The three and four atom gold clusters are also found to have similar losses in mass sensitivity with increasing temperature; $\Delta f = -16.3\%$ at 0.01 K for the three atom cluster but decreases to $\Delta f = -4.2\%$ at 300 K, while $\Delta f = -23.2\%$ at 0.01 K for the four atom cluster, and decreases to $\Delta f = -14.0\%$ at 300 K.

The preceding results strongly imply that the lack of mass sensitivity at elevated temperatures despite preventing the diffusion of the adsorbed atom is caused by another mechanism. The mechanism we now explore for the reduced mass sensitivity is the well-known reduction in Q-factor that occurs in nanostructures with increasing temperature [23, 24, 33, 36–39].

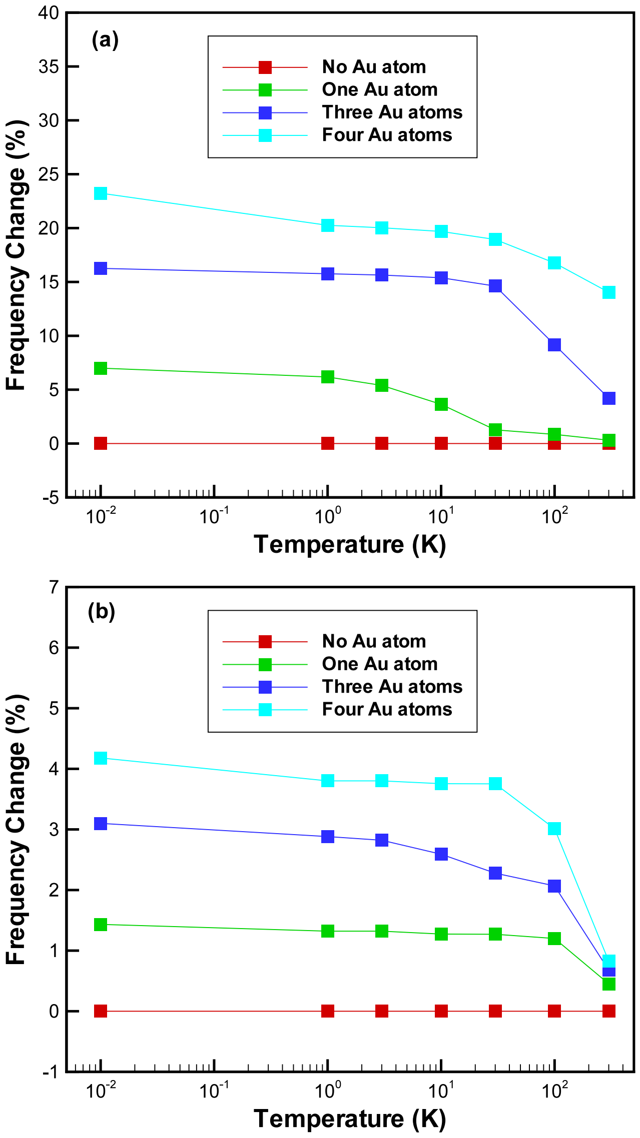

Figure 3. Change in frequency for an unstrained graphene monolayer with a single vacancy for one, three, and four adsorbed gold atoms at different temperatures as compared to a graphene monolayer with a single vacancy and no adsorbed mass for (a) small (547 carbon atom) model: defected graphene (strain 0.0%); (b) large (4886 carbon atom) model: defected graphene (strain 0.0%).

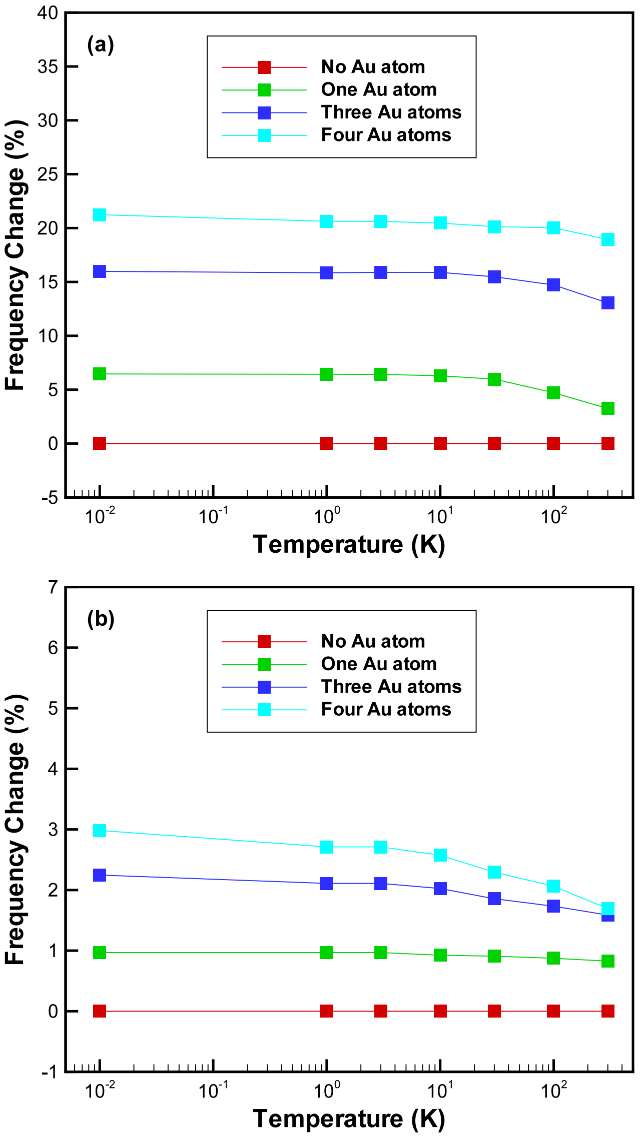

Figure 4. Change in frequency for a graphene monolayer under 1% tensile strain with a single vacancy for one, three, and four adsorbed gold atoms at different temperatures as compared to a graphene monolayer under 1% tensile strain with a single vacancy and no adsorbed mass for (a) small (547 carbon atom) model: defected graphene (strain 1.0%); (b) large (4886 carbon atom) model: defected graphene (strain 1.0%).

To determine if the Q-factor degradation with increasing temperature is responsible for the loss in mass sensitivity, we show in figures 4–6 the change in frequency for a graphene monolayer under 1, 2, or 3% tensile strain with a single vacancy for one, three, and four adsorbed gold atoms at different temperatures as compared to a graphene monolayer under 1, 2, or 3% tensile strain with a single vacancy and no adsorbed mass.

We briefly comment here on the amount of tensile mechanical strain we have applied to the graphene monolayer. The maximum tensile strain we applied was 3%; for comparison, previous MD simulations by Belytschko *et al* [40] of the tensile loading of single walled carbon nanotube found failure strains ranging from 10–15%. Similarly, Liu *et al* [41] recently performed *ab initio* calculations of the tensile loading of pristine graphene monolayers, and found that the failure strains for graphene depended on the loading direction, with the smallest failure strain being about 19%. Furthermore, researchers have recently demonstrated the experimental capability to apply up to 1% uniaxial strain to graphene sheets for strain-induced bandgap modification [42]. Overall, these results indicate that the amount of tensile strain (1–3%) we have utilized in the present work should not lead to any elastic instabilities in the graphene monolayer, either with or without defects.

Figures 4–6 show interesting results. In particular, they show that as the amount of applied tensile mechanical strain increases, the mass sensitivity of graphene monolayers with single atom vacancies can be sustained up to room temperatures (300 K), and that the mass sensitivity increases with an increase in applied strain; similar trends are observed

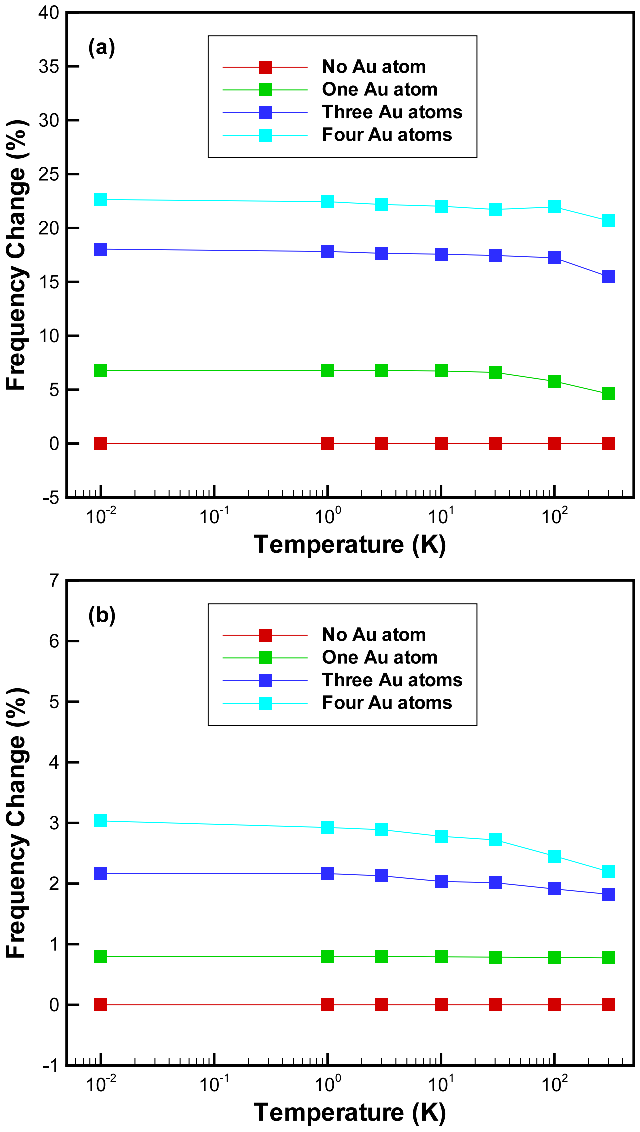

Figure 5. Change in frequency for a graphene monolayer under 2% tensile strain with a single vacancy for one, three, and four adsorbed gold atoms at different temperatures as compared to a graphene monolayer under 2% tensile strain with a single vacancy and no adsorbed mass for (a) small (547 carbon atom) model: defected graphene (strain 2.0%); (b) large (4886 carbon atom) model: defected graphene (strain 2.0%).

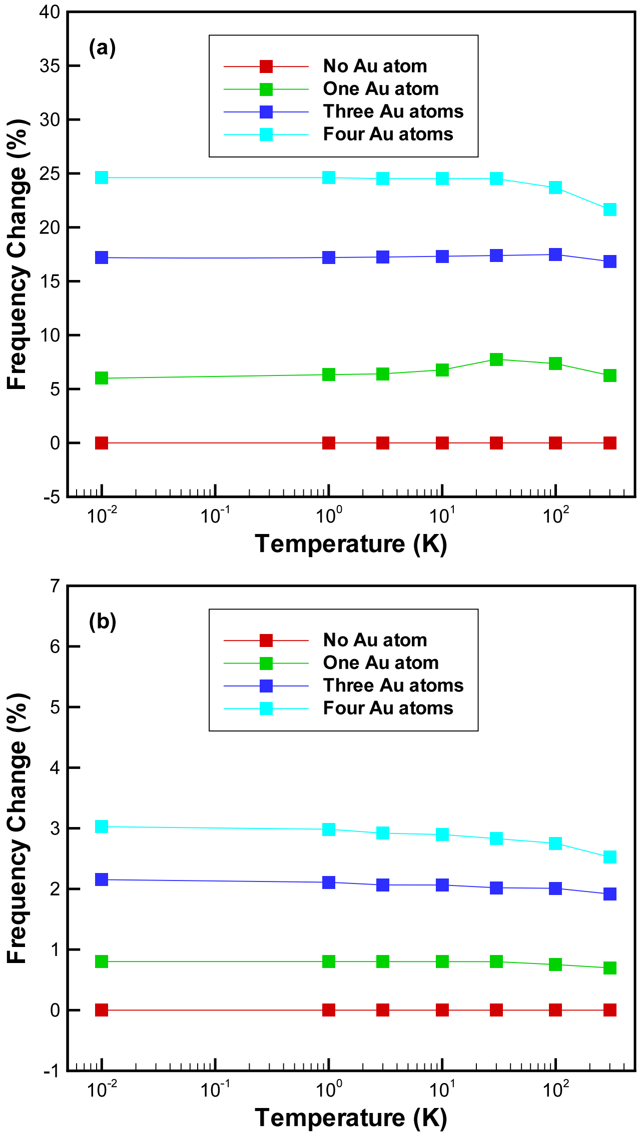

Figure 6. Change in frequency for a graphene monolayer under 3% tensile strain with a single vacancy for one, three, and four adsorbed gold atoms at different temperatures as compared to a graphene monolayer under 3% tensile strain with a single vacancy and no adsorbed mass for (a) small (547 carbon atom) model: defected graphene (strain 3.0%); (b) large (4886 carbon atom) model: defected graphene (strain 3.0%).

for both the small (547 carbon atom) and large (4886 carbon atom) graphene monolayers that were considered. In figure 4(a), which shows the results for the small graphene monolayer (547 carbon atoms) with a single atom vacancy under 1% tensile strain, the frequency shift for a single adsorbed gold atom decreases by about 50% between 0.01 and 300 K, i.e. $\Delta f = -6.46\%$ at 0.01 K and decreases to $\Delta f = -3.25\%$ at 300 K. While the 50% decrease in mass sensitivity is still quite large, this indicates that the mass sensitivity has not completely vanished, unlike the perfect graphene monolayer in figure 1 and the defective monolayer at 0% applied tensile strain in figure 3.

The mass sensing resolution can be further improved as observed in figure 5, where the graphene monolayer with a single vacancy has been stretched to 2% tensile strain; in figure 5(a) for the small graphene monolayer case, the change in the frequency shift for a single adsorbed gold atom is smaller than for the 1% tensile strain case, i.e. the frequency shift decreases by about 32%, from $\Delta f = -6.77\%$ at 0.01 K to $\Delta f = -4.61\%$ at 300 K.

Finally, through application of 3% tensile strain, as seen in figure 6, the frequency shift for a single adsorbed gold atom is found not to degrade between 0.01 and 300 K; $\Delta f = -6.00\%$ at 0.01 K and $\Delta f = -6.26\%$ at 300 K for the small graphene monolayer in figure 6 (a). Furthermore, similar performance is observed for the detection of three and four atom gold clusters; for the three atom gold cluster, $\Delta f = -17.19\%$ at 0.01 K and $\Delta f = -16.84\%$ at 300 K, while for the four atom gold cluster, $\Delta f = -24.61\%$ at 0.01 K and $\Delta f = -21.66\%$ at 300 K.

We therefore conclude that the key reason for the improvement in mass sensing resolution is the increase in Q-factor that occurs with increasing tensile mechanical strain; figures 4–6 have all demonstrated that the mass sensing resolution decreases with decreasing Q-factor (increasing temperature) for a fixed amount of applied tensile strain. In contrast, the mass sensing resolution is observed to increase with increasing mechanical strain for a given temperature. For concreteness, the Q-factor for the small graphene monolayer with a single vacancy was found to be about 2500 at 0% strain at 300 K, with an increase in Q up to 270 000 at 3% tensile strain at 300 K. According to equation (1), this 100 fold increase in room temperature Q-factor due to the application of tensile strain would enable the graphene monolayer to be able to detect masses that are ten times smaller.

Furthermore, it is seen through figures 4–6 that the increased mass sensitivity due to the increase in Q-factor with increasing tensile strain also leads to increased sensitivity to the same adsorbed atom, where the 3% tensile strained defected graphene monolayer in figure 6 maintains its sensitivity to one, three, or four adsorbed gold atoms due to its high Q-factor of nearly 300 000 seen in table 2. These results collectively indicate that by keeping the Q-factor acceptably high across a broad range of operating temperatures graphene monolayers with single atom vacancies can be utilized to detect individual gold atoms.

Before closing, we discuss the effect of the binding energy of the LJ potential between the carbon atoms surrounding the single atom vacancy and the adsorbed gold atom on the mass sensing potential of graphene. This was done in the present work for the small graphene monolayer at 1 K by varying the LJ binding energy between 100 times smaller and 100 times larger than the 2.62 eV binding energy calculated from DFT for gold to a single atom vacancy in graphite [28]. The low temperature was chosen to eliminate thermal fluctuations between the adsorbed gold atom and the defective graphene monolayer.

Figure 7 illustrates two interesting points. First, it shows that for a range of binding energies around ten times smaller (0.26 eV) and ten times larger (26.2 eV) than the gold–graphene vacancy value of 2.62 eV, the frequency shift due to an adsorbed mass stays relatively constant. However, for binding energies smaller than about 0.26 eV and larger than about 26.2 eV, the observed frequency shift due to a single adsorbed gold atom is found to increase. For the extreme upper end of binding energies, we suspect that the increased sensitivity results naturally from the strength of the bond between the carbon atoms surrounding the single atom vacancy and the adsorbed gold atom. For the extreme lower end of binding energies, we suspect that the increased sensitivity is due to increased fluctuations of the adsorbed gold atoms resulting from the weakness of the bond connecting the adsorbed gold atom to the carbon atoms surrounding the single atom vacancy in the graphene monolayer.

3. Conclusions

In conclusion, we have utilized classical MD simulations to study potential issues associated with mass sensing using graphene monolayers. We find that there are two distinct issues that must be overcome. First, we demonstrated that mass sensing resolution for pristine monolayer graphene is lost when the adsorbed atom diffuses at elevated temperatures. Second, we demonstrated that simply increasing the Q-factor of graphene does not resolve the loss of mass sensing resolution for a pristine graphene monolayer that occurs due to the diffusion of the adsorbed atom. Finally, we demonstrated that a combination of applied tensile mechanical strain, which significantly enhances the Q-factors of graphene, in conjunction with the introduction of single atom vacancies to enhance the binding between the adsorbed atom and the graphene monolayer to prevent diffusion, can lead to graphene retaining its mass sensing promise across a technologically relevant range of possible operating temperatures.

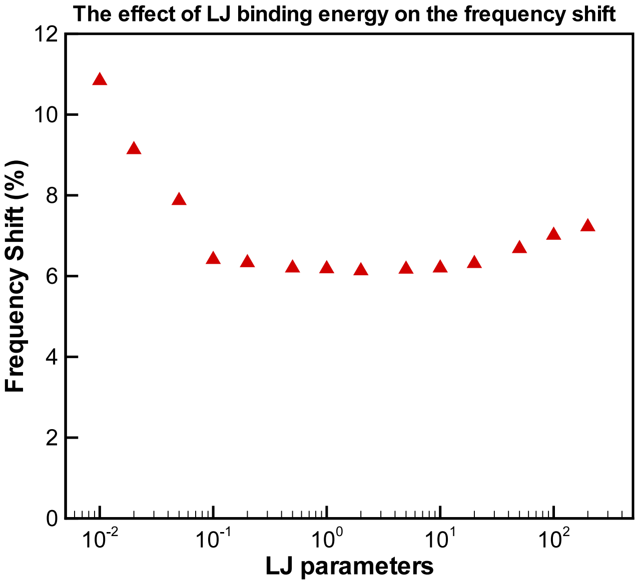

Figure 7. Effect of LJ potential binding energy upon the observed frequency shift for a single adsorbed gold atom on an unstrained small graphene monolayer (547 carbon atoms) with a single vacancy at a temperature of 1 K.

Acknowledgments

SYK and HSP both gratefully acknowledge the support of DARPA through grant HR0011-08-1-0047. The authors note that the content of this paper does not necessarily reflect the position or the policy of the government, and that no official government endorsement of the results should be inferred. HSP also acknowledges support from NSF grant CMMI-0750395. Both authors acknowledge Professor Sulin Zhang for sharing his Brenner potential code.

References

[1] Novoselov K S, Geim A K, Morozov S V, Jiang D, Katsnelson M I, Grigorieva I V, Dubonos S V and Firsov A A 2005 Two-dimensional gas of massless Dirac fermions in graphene *Nature* **438** 197–200

[2] Novoselov K S, Jiang D, Schedin F, Booth T J, Khotkevich V V, Morozov S V and Geim A K 2005 Two-dimensional atomic crystals *Proc. Natl Acad. Sci.* **102** 10451–3

[3] Geim A K and Novoselov K S 2007 The rise of graphene *Nat. Mater.* **6** 183–91

[4] Castro Neto A H, Guinea F, Peres N M R, Novoselov K S and Geim A K 2009 The electronic properties of graphene *Rev. Mod. Phys.* **81** 109–62

[5] Bunch J S, van der Zande A M, Verbridge S S, Frank I W, Tanenbaum D M, Parpia J M, Craighead H G and McEuen P L 2007 Electromechanical resonators from graphene sheets *Science* **315** 490–3

[6] Robinson J T, Zalalutdinov M, Baldwin J W, Snow E S, Wei Z, Sheehan P and Houston B H 2008 Wafer-scale reduced graphene oxide films for nanomechanical devices *Nano Lett.* **8** 3441–5

[7] Garcia-Sanchez D, van der Zande A M, San Paulo A, Lassagne B, McEuen P L and Bachtold A 2008 Imaging mechanical vibrations in suspended graphene sheets *Nano Lett.* **8** 1399–403

[8] Bunch J S, Verbridge S S, Alden J S, Van Der Zande A M, Parpia J M, Craighead H G and McEuen P L 2008 Impermeable atomic membranes from graphene sheets *Nano Lett.* **8** 2458–62

[9] Poncharal P, Wang Z L, Ugarte D and de Heer W A 1999 Electrostatic deflections and electromechanical resonances of carbon nanotubes *Science* **283** 1513–6

[10] Kong J, Franklin N R, Zhou C, Chapline M G, Peng S, Cho K and Dai H 2000 Nanotube molecular wires as chemical sensors *Science* **287** 622–5

[11] Peng H B, Chang C W, Aloni S, Yuzvinsky T D and Zettl A 2006 Ultrahigh frequency nanotube resonators *Phys. Rev. Lett.* **97** 087203

[12] Jensen K, Kim K and Zettl A 2008 An atomic-resolution nanomechanical mass sensor *Nat. Nanotechnol.* **3** 533–7

[13] Chiu H-Y, Hung P, Postma H W Ch and Bockrath M 2008 Atomic-scale mass sensing using carbon nanotube resonators *Nano Lett.* **8** 4342–6

[14] Ekinci K L and Roukes M L 2005 Nanoelectromechanical systems *Rev. Sci. Instrum.* **76** 061101

[15] Yang Y T, Callegari C, Feng X L, Ekinci K L and Roukes M L 2006 Zeptogram-scale nanomechanical mass sensing *Nano Lett.* **6** 583–6

[16] Ilic B, Craighead H G, Krylov S, Senaratne W, Ober C and Neuzil P 2004 Attogram detection using nanoelectromechanical oscillators *J. Appl. Phys.* **95** 3694–703

[17] Lee C, Wei X, Kysar J W and Hone J 2008 Measurement of the elastic properties and intrinsic strength of monolayer graphene *Science* **321** 385–8

[18] Robinson J T, Perkins F K, Snow E S, Wei Z and Sheehan P E 2008 Reduced graphene oxide molecular sensors *Nano Lett.* **8** 3137–40

[19] Ekinci K L, Yang Y T and Roukes M L 2004 Ultimate limits to inertial mass sensing based upon nanoelectromechanical systems *J. Appl. Phys.* **95** 2682–9

[20] Tamayo J, Ramos D, Mertens J and Calleja M 2006 Effects of the adsorbate stiffness on the resonance response of microcantilever sensors *Appl. Phys. Lett.* **89** 224104

[21] Li C and Chou T-W 2004 Mass detection using carbon nanotube-based nanomechanical resonators *Appl. Phys. Lett.* **84** 5246–8

[22] Sakhaee-Pour A, Ahmadian M T and Vafai A 2008 Applications of single-layered graphene sheets as mass sensors and atomistic dust detectors *Solid State Commun.* **145** 168–72

[23] Kim S Y and Park H S 2009 The importance of edge effects on the intrinsic loss mechanisms of graphene nanoresonators *Nano Lett.* **9** 969–74

[24] Kim S Y and Park H S 2009 Multilayer friction and attachment effects on energy dissipation in graphene nanoresonators *Appl. Phys. Lett.* **94** 101918

[25] Brenner D W, Shenderova O A, Harrison J A, Stuart S J, Ni B and Sinnott S B 2002 A second-generation reactive empirical bond order (REBO) potential energy expression for hydrocarbons *J. Phys.: Condens. Matter* **14** 783–802

[26] Anton R and Schneidereit I 1998 *In situ* TEM investigations of dendritic growth of Au particles on HOPG *Phys. Rev.* B **58** 13874–81

[27] Anton R and Kreutzer P 2000 *In situ* TEM evaluation of the growth kinetics of Au particles on highly oriented pyrolithic graphite at elevated temperatures *Phys. Rev.* B **61** 16077–83

[28] Akola J and Hakkinen H 2006 Density functional study of gold atoms and clusters on a graphite (0001) surface with defects *Phys. Rev.* B **74** 165404

[29] Malola S, Hakkinen H and Koskinen P 2009 Gold in graphene: in-plane adsorption and diffusion *Appl. Phys. Lett.* **94** 043106

[30] Cai J and Ye Y Y 1996 Simple analytical embedded-atom-potential model including a long-range force for fcc metals and their alloys *Phys. Rev.* B **54** 8398–410

[31] Hoover W G 1985 Canonical dynamics: equilibrium phase-space distributions *Phys. Rev.* A **31** 1695–7

[32] Verbridge S S, Shapiro D F, Craighead H G and Parpia J M 2007 Macroscopic tuning of nanomechanics: substrate bending for reversible control of frequency and quality factor of nanostring resonators *Nano Lett.* **7** 1728–35

[33] Kim S Y and Park H S 2008 Utilizing mechanical strain to mitigate the intrinsic loss mechanisms in oscillating metal nanowires *Phys. Rev. Lett.* **101** 215502

[34] Dai M C, Eom K and Kim C-W 2009 Nanomechanical mass detection using nonlinear oscillations *Appl. Phys. Lett.* **95** 203104

[35] Verbridge S S, Parpia J M, Reichenbach R B, Bellan L M and Craighead H G 2006 High quality factor resonance at room temperature with nanostrings under high tensile stress *J. Appl. Phys.* **99** 124304

[36] Jiang H, Yu M F, Liu B and Huang Y 2004 Intrinsic energy loss mechanisms in a cantilevered carbon nanotube beam oscillator *Phys. Rev. Lett.* **93** 185501

[37] Evoy S, Olkhovets A, Sekaric L, Parpia J M, Craighead H G and Carr D W 2000 Temperature-dependent internal friction in silicon nanoelectromechanical systems *Appl. Phys. Lett.* **77** 2397–9

[38] Roukes M L 2001 Nanomechanical systems face the future *Phys. World* **14** 25–31

[39] Carr D W, Evoy S, Sekaric L, Craighead H G and Parpia J M 1999 Measurement of mechanical resonance and losses in nanometer scale silicon wires *Appl. Phys. Lett.* **75** 920–2

[40] Belytschko T, Xiao S P, Schatz G C and Ruoff R S 2002 Atomistic simulations of nanotube fracture *Phys. Rev.* B **65** 235430

[41] Liu F, Ming P and Li J 2007 *Ab initio* calculation of ideal strength and phonon instability of graphene under tension *Phys. Rev.* B **76** 064120

[42] Ni Z H, Yu T, Lu Y H, Wang Y Y, Feng Y P and Shen Z X 2008 Uniaxial strain on graphene: Raman spectroscopy study and band-gap opening *ACS Nano* **2** 2301–5